The Plant Cell, Vol. 29: 560–574, March 2017, www.plantcell.org

ABNORMAL INFLORESCENCE MERISTEM1 Functions in Salicylic Acid Biosynthesis to Maintain Proper Reactive Oxygen Species Levels for Root Meristem Activity in Rice

Lei Xu,[a,b,1] Hongyu Zhao,[a,b,1] Wenyuan Ruan,[b,1] Minjuan Deng,[c] Fang Wang,[c] Jinrong Peng,[a] Jie Luo,[d] Zhixiang Chen,[e] and Keke Yi[b,c,2]

[a] College of Life Sciences, Zhejiang University, Hangzhou 310058, China
[b] Key Laboratory of Plant Nutrition and Fertilizers, Ministry of Agriculture, Institute of Agricultural Resources and Regional Planning, Chinese Academy of Agricultural Sciences, Beijing 10081, China
[c] The State Key Laboratory Breeding Base for Sustainable Control of Pest and Disease, Institute of Virology and Biotechnology, Zhejiang Academy of Agricultural Sciences, Hangzhou 310021, China
[d] College of Life Sciences and Technology, Huazhong Agricultural University, Wuhan 430070, China
[e] Department of Botany and Plant Pathology, Purdue University, West Lafayette, Indiana 47907

ORCID IDs: 0000-0003-4157-0686 (L.X.); 0000-0002-3916-477X (K.Y.)

Root meristem activity determines root growth and root architecture and consequently affects water and nutrient uptake in plants. However, our knowledge about the regulation of root meristem activity in crop plants is very limited. Here, we report the isolation and characterization of a short root mutant in rice (*Oryza sativa*) with reduced root meristem activity. This root growth defect is caused by a mutation in *ABNORMAL INFLORESCENCE MERISTEM1* (*AIM1*), which encodes a 3-hydroxyacyl-CoA dehydrogenase, an enzyme involved in β-oxidation. The reduced root meristem activity of *aim1* results from reduced salicylic acid (SA) levels and can be rescued by SA application. Furthermore, reduced SA levels are associated with reduced levels of reactive oxygen species (ROS) in *aim1*, likely due to increased expression of redox and ROS-scavenging-related genes, whose increased expression is (at least in part) caused by reduced expression of the SA-inducible transcriptional repressors WRKY62 and WRKY76. Like SA, ROS application substantially increased root length and root meristem activity in *aim1*. These results suggest that AIM1 is required for root growth in rice due to its critical role in SA biosynthesis: SA maintains root meristem activity through promoting ROS accumulation by inducing the activity of WRKY transcriptional repressors, which repress the expression of redox and ROS-scavenging genes.

INTRODUCTION

Plant roots are exposed to rapidly changing environments, including drought and nutrient deficiency. To cope with the ever-changing environment, plants modulate their root growth and architecture for better uptake of water and nutrients. Root growth and development require the continuous production of new cells by stem cells. The progeny of these stem cells rapidly divide in a transit-amplifying zone known as the meristem and enter the elongation/differentiation zone, where they start to differentiate. Root meristem activity is a key determinant of root growth and architecture. To ensure root meristem maintenance, the rates of cell division and differentiation must be coordinated: disrupting this balance affects root meristem activity and, thus, root size. The mechanism underlying the regulation of root meristem activity in crop plants is largely unknown.

In the *Arabidopsis thaliana* root meristem, several factors affecting the balance between cell division and cell differentiation are involved in regulating root meristem activity. A distal auxin maximum helps regulate root pattern formation and the extent of cell division (Sabatini et al., 1999). This auxin gradient is believed to control root growth by regulating the expression of *PLETHORA*s (*PLTs*) (Galinha et al., 2007). A complex network of interactions of hormonal pathways also plays a pivotal role in the regulation of root growth. For example, the interaction between cytokinin and auxin determines the size of the meristem. These hormonal interactions are thought to determine root meristem size through the regulation of genes involved in auxin signaling and/or transport to ensure the appropriate distribution of the auxin gradient (reviewed in Pacifici et al., 2015). In addition, reactive oxygen species (ROS) play a role in regulating meristem size in Arabidopsis. ROS are normally generated as by-products of aerobic respiration, but they play important signaling roles in all living organisms, including plants. As a result, ROS are important for processes such as growth, development, and responses to biotic and abiotic environmental stimuli. In plants, root tips represent a zone of active ROS production (Liszkay et al., 2004). The distribution of superoxide and hydrogen peroxide in the root tip has been analyzed in Arabidopsis (Dunand et al., 2007). Environmental stresses arising from the rhizosphere also affect the accumulation of ROS in the plant root. For example, mechanical and nutrient deficiency stress from the soil can lead to an alteration in ROS levels in the root tip, affecting the direction and extent of root growth (Sánchez-Fernández et al., 1997). During this process, hormones are also important for maintaining ROS homeostasis in the root, as an asymmetric distribution of auxin can affect both ROS

[1] These authors contributed equally to this work.
[2] Address correspondence to yikeke@gmail.com.
The author responsible for distribution of materials integral to the findings presented in this article in accordance with the policy described in the Instructions for Authors (www.plantcell.org) is: Keke Yi (yikeke@gmail.com or yikeke@caas.cn)
www.plantcell.org/cgi/doi/10.1105/tpc.16.00665

states and root gravitropism (Joo et al., 2001). A few genetic factors have been shown to affect ROS and redox homeostasis in the root tip during root growth. In Arabidopsis, UPBEAT1 (UPB1), a bHLH transcription factor, regulates the balance between superoxide and hydrogen peroxide by directly repressing peroxidase expression in the elongation zone. *UPB1* mutants have longer roots than wild-type plants, a phenotype associated with reduced hydrogen peroxide and increased superoxide levels in the root tip. The UPB1-regulated root development process appears to be independent of the auxin signaling pathway (Tsukagoshi et al., 2010). GLUTATHIONE REDUCTASE2, a glutathione biosynthetic enzyme, regulates glutathione redox status to maintain meristem activity and root growth (Yu et al., 2013). However, how phytohormones regulate ROS homeostasis to help maintain root meristem activity is still largely unknown.

The β-oxidation pathway is a catabolic process by which a fatty acid is metabolized to generate acetyl-CoA. The process of β-oxidation is common to all prokaryotic and eukaryotic organisms. Eukaryotes have two major β-oxidation systems, mitochondrial and peroxisomal. Plant peroxisomes are the sole site of fatty acid β-oxidation. The core pathway of peroxisomal β-oxidation undergoes a cycle of oxidation, hydration, oxidation, and thiolysis. The first step is catalyzed by a family of ACYL-CoA OXIDASES, which require flavin adenine dinucleotide and produce H_2O_2. The two subsequent steps are catalyzed by MULTIFUNCTIONAL PROTEINs (MFPs), which exhibit hydratase, dehydrogenase, epimerase, and isomerase activities. The last step of the cycle is catalyzed by L-3-KETOACYL-CoA THIOLASE, which cleaves off acetyl-CoA, thereby shortening the original acyl-CoA by two carbon atoms (Goepfert and Poirier, 2007). The Arabidopsis genome contains two isoforms of MFP, ABNORMAL INFLORESCENCE MERISTEM1 (AIM1) and MFP2. Mutations in *AIM1* lead to abnormal vegetative and reproductive development (Richmond and Bleecker, 1999), while *MFP2* mutants exhibit sucrose-dependent seedling establishment. A complete block in β-oxidation via the introduction of the *aim1 mfp2* double mutation causes early embryonic lethality (Rylott et al., 2006). In addition to its role in fatty acid catabolism, peroxisomal β-oxidation is required for the metabolism of hormones and amino acids (reviewed in Baker et al., 2006). Although the roles of the enzymes involved in β-oxidation have been extensively studied in Arabidopsis, their roles in other plants such as rice (*Oryza sativa*) that do not accumulate high levels of triacylglycerols, the major form of storage fatty acids, are unclear.

Here, we investigated the role of AIM1 in root meristem activity maintenance and root growth in rice. We found that salicylic acid (SA) biosynthesis in rice roots is dependent on AIM1. AIM1-dependent SA biosynthesis is required for the maintenance of root meristem activity. Our results suggest that SA represses the expression of redox and ROS scavenging-related genes to maintain ROS accumulation for root meristem activity, partially through the activity of the transcriptional repressors WRKY62 and WRKY76.

RESULTS

Rice *aim1* Is a Short Root Mutant with Reduced Root Meristem Activity

To identify genes affecting root meristem activity in rice, we tried to isolate short root mutants by screening a mutagenized rice population generated through treating seeds of rice cultivar Shishoubaimao (*O. sativa* ssp japonica) with ^{60}Co-ray radiation. After screening around 30,000 M_2 seeds, a short root mutant was identified, which was designated *aim1* based on our subsequent characterization of the mutant gene (Figure 1A). The lengths of seedling roots and adventitious roots in *aim1* are significantly shorter than those of wild-type plants, while the lateral root length of the mutant is comparable to that of the wild type (Supplemental Figure 1B). To characterize the root growth defects in the *aim1* mutant, we compared the root growth rates between the wild type and the mutant and found that the short root phenotype of *aim1* is due to a reduced growth rate but not to an early cessation of root growth (Figure 1B). Based on images of longitudinal and transversal sections of wild-type and *aim1* seedling roots, the radial patterning and meristem organization of the mutant were similar to those in the wild type, and there were no obvious defects in the quiescent center (QC) of the stem cell niche in *aim1*. The cortex layer and formation of aerenchyma (spongy tissue with air spaces) in the mutant roots were also normal (Figures 1C and 1D; Supplemental Figure 1A). Measurement of the root meristem length showed that the meristem size of *aim1* was reduced (Figure 1E). The mature cortical cell length in *aim1* roots was slightly shorter than that of the wild type (Figure 1F). These findings indicate that the short root defect of *aim1* primarily results from reduced meristem activity. To determine the root meristem activity of the mutant, we cultured 4-d-old seedlings for 2 h in the presence of the thymidine analog 5-ethynyl-2′-deoxyuridine (EdU) and visualized the in situ incorporation of EdU into DNA during active DNA synthesis in cells at the S-phase in the root tip (Kotogány et al., 2010). Compared with the wild type, the *aim1* mutant had reduced levels of EdU labeling in the root meristem (Figure 1G). We also determined the expression of *CYCLINB1;1* (*CYCB1;1*), a marker for the G2-M phase transition, in the *aim1* mutant and found that its transcript levels in the mutant were significantly lower than those in the wild type. Taken together, these results indicate that the root meristem activity of the *aim1* mutant is compromised.

AIM1 Encodes a 3-Hydroxyacyl-CoA Dehydrogenase Involved in β-Oxidation

To identify the mutated gene, we developed an F2 population by crossing *aim1* with Kasalath, an indica-type rice cultivar, followed by map-based cloning. The segregation of the short root phenotype in the F2 population displayed a ratio close to 3:1, with 119 plants of the wild-type phenotype and 35 plants of the *aim1* phenotype ($\lambda^2 = 0.42$; $P < 0.05$), suggesting that a single recessive gene was responsible for the mutant phenotype. Using PCR-based molecular markers, the mutation was mapped to an ~168-kb region between molecular markers S2-9925K and S2-10093K on chromosome 2. We amplified and sequenced putative coding regions of the 22 genes in this region from *aim1*. Only a 26-bp deletion of the Os02g17390 coding region (202 bp from the start codon) was identified (Figure 2A), which would alter codons after amino acid residue 68 and introduce a premature stop codon in the gene. Os02g17390 encodes a putative 3-hydroxyacyl-CoA dehydrogenase, which is a homolog of Arabidopsis AIM1 (Richmond and Bleecker, 1999). Rice *AIM1* contains 18 exons and 17 introns. The full-length open reading frame

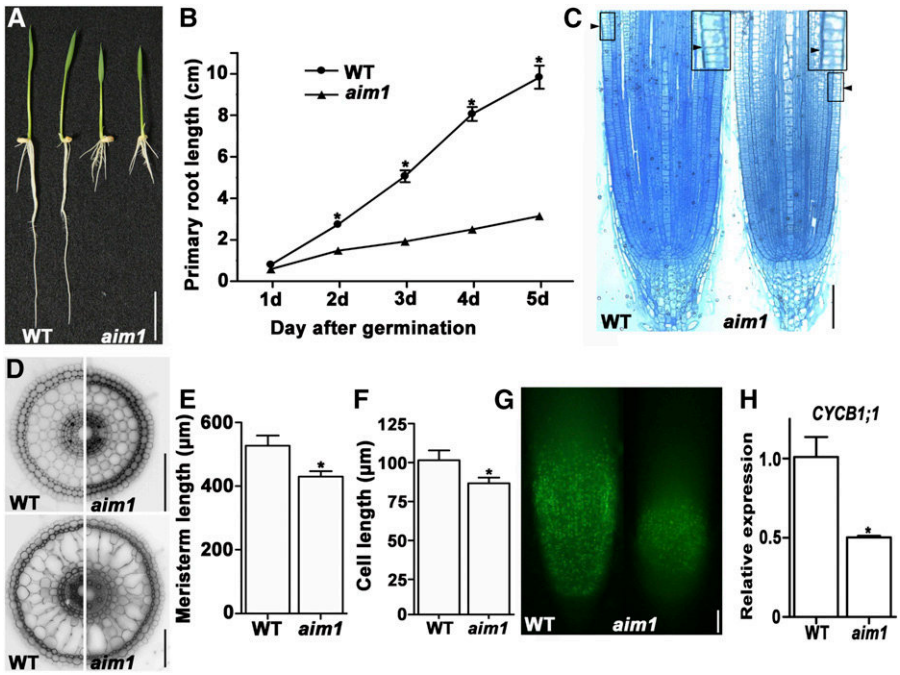

Figure 1. *aim1* Is a Short Root Mutant with Reduced Meristem Activity.

(A) Root phenotype of 4-d-old wild type and *aim1*. Bar = 2 cm.
(B) Time course of primary root length of wild-type and *aim1* seedlings after germination. Error bars represent SD (n = 10).
(C) Longitudinal sections of wild-type and *aim1* root tips. Arrowheads indicate the proximal end of the root meristem. Insets are an enlargement of the regions at the proximal end of the root meristem. Bar = 100 μm.
(D) Transverse sections of the wild type and *aim1* in the root mature zone (top panel: root hair initiation region; lower panel: aerenchyma formation region). Bar = 100 μm.
(E) Meristem length of 4-d-old wild type and *aim1* (from the quiescent center to the start of the elongation zone). Error bars represent SD (n = 20).
(F) Longitudinal cell length of cortical cells in the mature region of the root. Error bars represent SD (n = 30).
(G) S-phase entry of 4-d-old wild-type and *aim1* root tips visualized by EdU staining. Bar = 100 μm.
(H) Relative expression of *CYCB1;1* in root tips of 4-d-old wild-type and *aim1*. The expression level was compared with that in the wild type. Total RNA was collected from the 2.5-mm root apex of seedlings. Three biological replicates were performed. Samples were collected from three independent experiments. The asterisks in **(B)**, **(E)**, **(F)**, and **(H)** indicate a significant difference between the wild type and *aim1* ($P < 0.01$, by Student's t test).

is 2181 bp long and encodes a 726-amino acid protein. Rice AIM1 belongs to the MFP family. The rice genome contains four MFPs. Multiple sequence alignment and phylogenetic analysis of the plant MFP proteins indicated that the MFPs can be divided into two subclades, the AIM1 clade and the MFP2 clade. *AIM1* is the only gene that belongs to the AIM1 subclade in the rice genome (Figure 2B; Supplemental File 1). In Arabidopsis, the *aim1* mutant displays abnormal inflorescence meristems (Richmond and Bleecker, 1999). However, the panicle of *aim1* is largely normal in rice (Supplemental Figure 1C), indicating that Os-*AIM1* might function differently from the Arabidopsis homolog At-*AIM1*.

To confirm that the 26-bp deletion in *aim1* is responsible for the mutant phenotype, we transformed *aim1* plants with a binary vector containing the 2181-bp *AIM1* coding sequence driven by either the *AIM1* promoter or the *CaMV 35S* promoter. Over 20 individual lines were obtained for each construct; lines with normal or elevated *AIM1* expression all showed restoration of normal root growth (Figure 2C; Supplemental Figures 1D and 1E). This result indicates that the short root phenotype in *aim1* is caused by the 26-bp deletion in *AIM1*.

Subcellular Localization and Tissue Expression Pattern of AIM1

As AIM1 is a multifunctional protein, it was predicted to be a peroxisomal protein. To determine the subcellular localization of AIM1, we introduced the *Pro35S:GFP-AIM1* construct and a peroxisomal marker (mCherry-PTS1) (Nelson et al., 2007) into rice protoplasts for transient coexpression. Confocal microscopy revealed randomly distributed punctate GFP-AIM1 signals that colocalized with those of peroxisome-targeted mCherry-PTS1, confirming the peroxisomal localization of AIM1 (Figure 3A).

To determine the tissue-specific expression pattern of *AIM1*, we performed quantitative RT-PCR analysis of the expression of the MFPs in various rice tissues and found that *AIM1* had the second highest expression level in root tissues among the four MFP genes (Supplemental Figure 2). We then generated *ProAIM1:GUS-AIM1* transgenic lines to analyze the expression pattern of *AIM1*. The *GUS-AIM1* fusion driven by its native promoter completely rescued the *aim1* root growth defects (Supplemental Figure 3), indicating that the fusion protein is fully functional. We performed

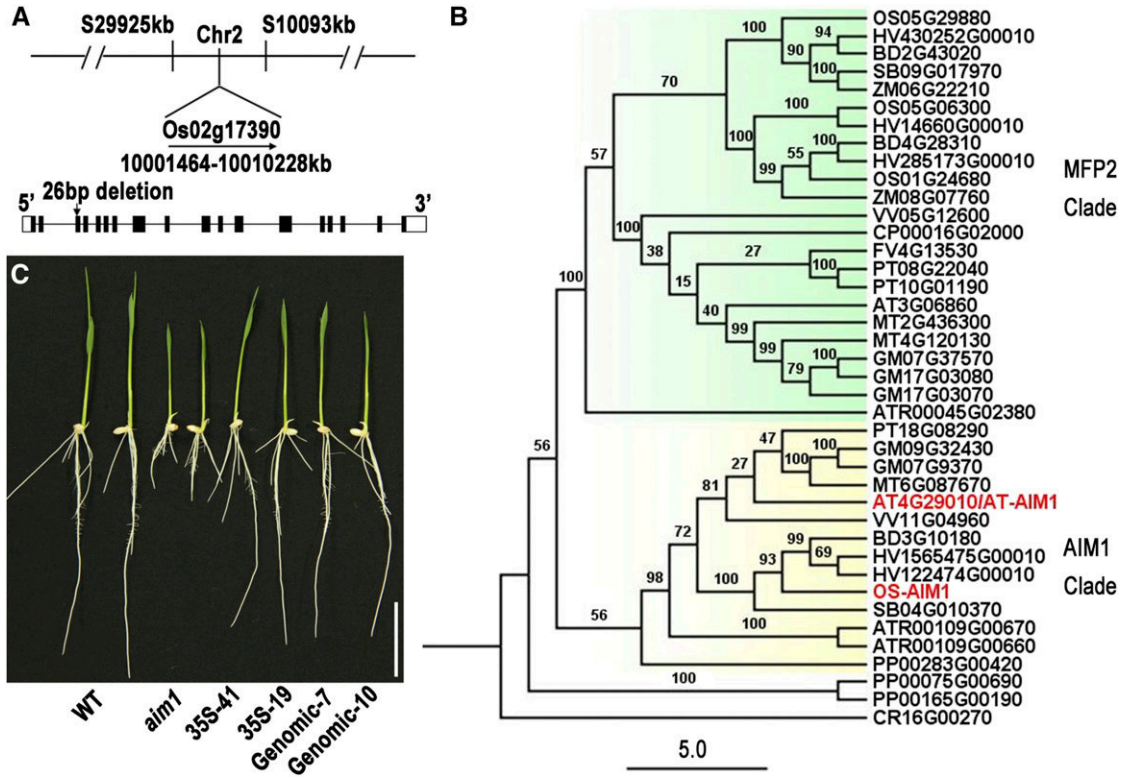

Figure 2. *AIM1* Encodes a 3-Hydroxyacyl-CoA Dehydrogenase.

(A) Map-based cloning of *AIM1*. Black boxes represent exons. Lines between boxes represent introns. White boxes represent untranslated region. Arrow shows the site of the 26-bp deletion from nucleotides 202 to 227 bp downstream of ATG.

(B) Phylogenetic tree of the MFP family. Bootstrap values from 1000 replicates are indicated at each branch. ATR, *Amborella trichopoda*; FV, *Fragaria vesca*; GM, *Glycine max*; MT, *Medicago truncatula*; AT, *Arabidopsis thaliana*; PT, *Populus trichocarpa*; CP, *Carica papaya*; VV, *Vitis vinifera*; HV, *Hordeum vulgare*; BD, *Brachypodium distachyon*; OS, *Oryza sativa*; SB, *Sorghum bicolor*; ZM, *Zea mays*; PP, *Physcomitrella patens*; CR, *Chlamydomonas reinhardtii*.

(C) Complementation of the short root defect of *aim1* by transformation with *Pro35S:AIM1* (35S) and *ProAIM1:AIM1* (Genomic); two individual lines per construct are shown. Bar = 2 cm.

detailed analysis of the GUS expression patterns of the *ProAIM1:GUS-AIM1* lines. GUS staining was detected in the cells of the lateral root cap and the epidermis and the stele in the root but not in quiescent center cells (Figures 3F to 3H). In the mature zone, GUS staining was detected in the root hairs, exodermis, stele, endodermis, and cortex adjacent to the endodermis (Figures 3D and 3E). Strong GUS activity was also ubiquitously detected in leaf cells (Figures 3B and 3C).

AIM1-Dependent SA Biosynthesis Is Required for Root Meristem Activity

To elucidate the metabolic pathway that is defective in *aim1* and causes its short root phenotype, we measured the levels of indole-3-acetic acid (IAA) and jasmonic acid (JA) in the mutant. Consistent with the role of β-oxidation in JA biosynthesis, the JA levels in the mutant were only 15% those of the wild type (Supplemental Figure 4A). However, the IAA levels in the mutant were comparable to those of the wild type (Supplemental Figure 4B). To determine whether reduced JA levels caused the short root phenotype of *aim1*, we applied JA to the mutant but found no restoration of the root growth of the mutant after supplementation with JA (Supplemental Figure 4C). In fact, the application of the JA biosynthesis inhibitor, diethyldithiocarbamate trihydrate (DIECA), slightly increased root elongation in both the wild type and *aim1* (Supplemental Figure 4D), indicating that JA is an inhibitor, not a promoter, of root growth in rice. This observation is consistent with the previous finding that the exogenous application of JA inhibits root meristem activity through the repression of *PLT1* and *PLT2* expression in Arabidopsis (Chen et al., 2011). Therefore, we conclude that the short root defect of *aim1* did not resulted from compromised IAA and JA biosynthesis or signaling.

Recently, AIM1 was shown to be required for SA biosynthesis in Arabidopsis seeds (Bussell et al., 2014). Therefore, we also measured the SA levels and found that they were significantly reduced in *aim1* roots compared with the wild type (Figure 4A). To determine whether the defect in SA biosynthesis in the mutant is due to the mutation of *AIM1*, we also measured the SA contents of the complementation lines. We found that their SA levels were restored to wild-type levels by introducing the *AIM1* gene driven by either its native promoter or the *CaMV 35S* promoter in

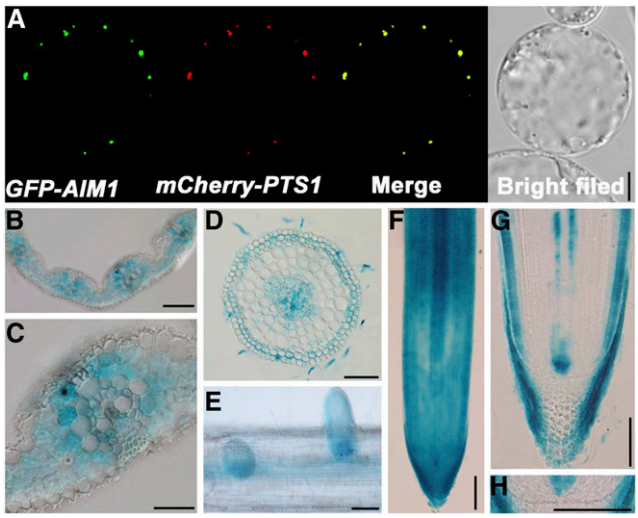

Figure 3. The Peroxisomal Localization and Expression Pattern of AIM1.

(A) GFP-AIM1 colocalizes with the peroxisomal marker mCherry-PTS1 (red) in rice protoplasts. Bar = 50 μm.
(B) to **(H)** The expression of GUS-AIM1 in different tissues.
(B) Section of leaf blade. Bar = 100 μm.
(C) Vascular bundle of leaf blade. Bar = 50 μm.
(D) Transverse section of primary root. Bar = 50 μm.
(E) Lateral root. Bar = 100 μm.
(F) Primary root tip. Bar = 100 μm.
(G) Longitudinal section of primary root tip. Bar = 100 μm.
(H) Section of primary root initial region. Bar = 100 μm.

complementation lines (Supplemental Figure 5A). Thus, AIM1 is required for SA biosynthesis in rice.

SA is thought to be synthesized from cinnamic acid (CA) via benzoic acid (BA) in rice (Silverman et al., 1995). β-Oxidation is required for the shortening of the side chain of CA to produce BA. Given the role of AIM1 in SA biosynthesis in rice, we analyzed the levels of SA precursors in the wild type and the *aim1* mutant. Our results showed that in addition to SA, there was a significant reduction in BA levels in the mutant (Figure 4A). By contrast, the levels of CA, the putative substrate for β-oxidation, were greatly elevated in the mutant compared with the wild type (Figure 4A). These results are consistent with a role of AIM1 in the conversion of BA from CA.

To further confirm the role of AIM1 in SA biosynthesis, we performed chemical feeding experiments. Feeding wild-type plants with 250 μM CA for 48 h resulted in an ~9-fold increase in BA levels, but the *aim1* mutant fed with CA exhibited less than 40% of wild-type BA levels (Supplemental Figure 5B). Likewise, feeding with CA led to an ~6-fold increase in SA levels in wild-type plants but only about a 1-fold increase in *aim1* (Supplemental Figure 5C). By contrast, feeding with BA resulted in similar levels of SA in wild-type and *aim1* mutant plants (Supplemental Figure 5C). Collectively, these results strongly suggest that AIM1-dependent β-oxidation is critical for the conversion of BA from CA in the SA biosynthetic pathway in rice.

To determine whether the short root phenotype of *aim1* results from the reduced SA levels in seedlings, we treated the plants with SA and found that the exogenous application of SA rescued the short root defect of *aim1*, although the SA treatments inhibited the root elongation of the wild type in a dosage-dependent manner (Figure 4B; Supplemental Figure 6A). The exogenous application of methyl salicylate also rescued the root growth defects of *aim1* (Supplemental Figure 6B). Consistent with the restoration of root elongation in *aim1*, EdU labeling demonstrated that the application of SA fully rescued the root meristem activity of the mutant (Figure 4C). Furthermore, after SA treatment, we observed no significant difference in root cortical cell length between the wild type and *aim1* (Figure 4D). Based on these results, we conclude that AIM1 is required for the biosynthesis of SA at a sufficient level for maintaining root meristem activity in rice.

SA Biosynthesis Is Critical for the Regulation of Genes Associated with Redox Homeostasis and ROS Scavenging in the Rice Root Tip

To further determine the possible role of SA in root meristem activity, we compared the gene expression profiles of the root tips of *aim1* and the wild type with or without SA treatment using Affymetrix arrays. Without SA treatment, ~3555 genes showed >2-fold difference in expression level between the wild type and *aim1* mutant (false discovery rate of 5%), with 2821 upregulated and 734 downregulated genes in the *aim1* background. Consistent with the rescue of the root growth defects of *aim1* by SA application, the expression of 90% of the differentially expressed genes (2533 of the upregulated genes and 709 of the downregulated genes) was restored to wild-type levels in the *aim1* after SA treatment (Figure 5A). To verify the data from microarray analysis, we selected a number of differentially expressed genes for qRT-PCR analysis and found that the qRT-PCR results were in general agreement with the microarray data (Figure 5B).

To further analyze the effects of SA on the transcriptomes, we performed Gene Ontology (GO) classification analysis of the 709 AIM1-dependent genes (Supplemental Table 1). The analysis showed that genes encoding proteins involved in transferring glycosyl groups and with xyloglucan:xyloglucosyltransferase activity were enriched among AIM1-dependent differentially expressed genes (P = 4.9E-06). These genes are involved in cell wall organization and therefore may play a role in cell division. Several *CYCLIN* genes (*CYCB1;1*, *CYCB1;2*, *CYCB1;4*, *CYCB2;2*, *CYCD2;2*, and *CYCD6;1*) were among these AIM1-dependent genes, as their expression was also reduced in the *aim1* mutant without SA treatment. SA application induced the expression of these cyclin genes in the *aim1* background to levels similar to those in the wild type (Supplemental Table 2). This finding further supports the positive role of SA in root meristem activity. SA is a hormone involved in plant defense, and we also noticed that a number of *PATHOGENESIS-RELATED* (*PR*) genes were upregulated in the *aim1* mutant background and that this upregulation was repressed by exogenous SA application (Figure 5B; Supplemental Table 3). We also performed GO classification analysis of the 2533 AIM1-repressed genes whose expression in the *aim1* mutant was upregulated without SA treatment but was similar to that of the wild type after SA treatment (Supplemental Table 1). Importantly, a substantial number of genes in the categories oxidoreductase (P = 3.7 E -07), glutathione transferase

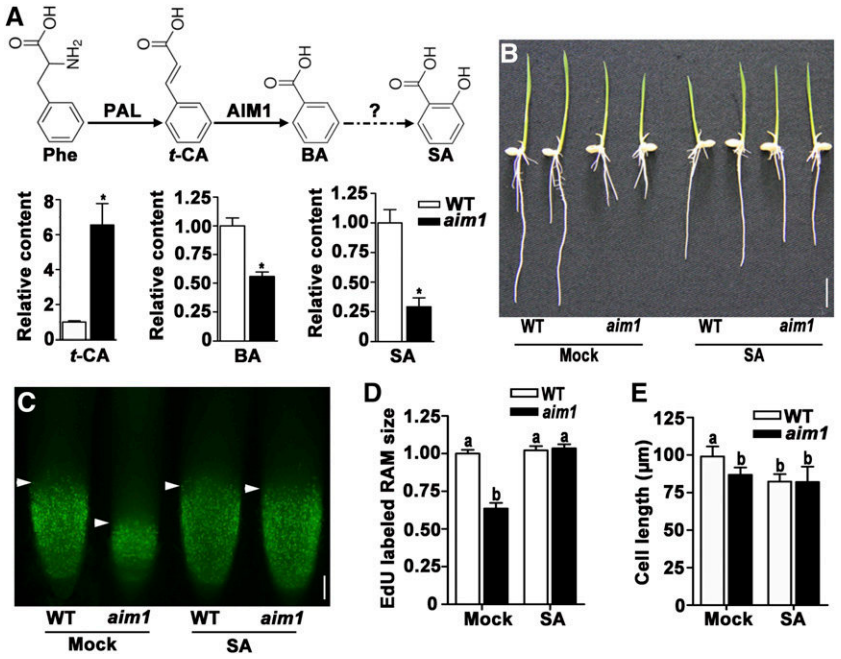

Figure 4. The Root Meristem Activity Defect in *aim1* Results from Deficient SA Biosynthesis.

(A) The possible SA biosynthesis pathway in rice and the relative contents of CA, BA, and SA in wild-type and *aim1* roots. The asterisk indicates a significant difference ($P < 0.01$, by Student's *t* test). Error bars represent SD ($n = 3$). *t*-CA, *trans*-cinnamic acid; PAL, phenylalanine ammonia lyase.

(B) Phenotype of 4-d-old wild type and *aim1* grown on mock medium and medium supplemented with 0.5 mM SA. Bar = 1 cm.

(C) Representative S-phase entry of root tip cells of 4-d-old wild type and *aim1* in **(B)** visualized by EdU staining. The arrowheads indicate the border of the EdU staining signal. Bar = 100 μm.

(D) Sizes of EdU-labeled RAMs (root apical meristems) shown in **(C)**. Error bars represent SD ($n = 8$).

(E) Longitudinal cell length of cortical cells in the mature region of wild-type and *aim1* roots grown on mock medium and medium supplemented with 0.5 mM SA. Error bars represent SD ($n = 30$). Different letters in **(D)** and **(E)** indicate a significant difference ($P < 0.01$, by Tukey's test).

activities ($P = 2.4$ E-05), and antioxidants ($P = 0.00077$) were highly enriched in the gene list, suggesting that the defect in SA biosynthesis in *aim1* altered the expression of redox and ROS scavenging-related genes. For example, METALLOTHIONEINs are ROS scavengers in plants (reviewed in Hassinen et al., 2011). In this study, four members of the *METALLOTHIONEIN* gene family were expressed in root tissue at higher levels in *aim1* root tips than in the wild type under normal conditions. Again, SA application led to a reduction in the expression of these *METALLOTHIONEIN* genes in the mutant. CATALASEs catalyze the decomposition of hydrogen peroxide (Scandalios et al., 1997), and we found that two *CATALASE* genes were upregulated and that SA application reduced their expression in the *aim1* mutant.

ALTERNATIVE OXIDASE (AOX) is a mitochondria enzyme that can lower mitochondrial ROS accumulation in the cell (Maxwell et al., 1999). We therefore generated a construct harboring the GUS reporter gene driven by the rice AOX gene promoter (*ProAOX1a:GUS*) and introduced it into wild-type and *aim1* plants. Similar to the results of transcriptome analysis, the expression of *ProAOX1a:GUS* in the root tip was much stronger in the *aim1* background than in the wild type (Figure 5C). Again, the difference between the wild type and *aim1* mutant in terms of the levels of *ProAOX1a:GUS* expression was suppressed by SA treatment (Figure 5C). Tree view (heat map) analysis of many genes associated with redox and ROS scavenging identified from transcriptome analysis showed that their differential expression levels in wild-type and *aim1* plants were largely reduced after SA treatment (Figure 5D). Thus, reduced SA accumulation in the *aim1* mutant resulted in increased expression of genes related to redox and ROS scavenging. These results indicate that SA biosynthesis in rice roots negatively regulates the expression of redox and ROS scavenging-related genes, which could further affect ROS accumulation in the root tip.

AIM1 Is Required for SA Biosynthesis to Maintain ROS Levels in Rice Root

To investigate whether ROS levels were also altered in *aim1*, we measured ROS levels in *aim1* root tip using 3′-(ρ-hydroxyphenyl) fluorescein (HPF) and nitro blue tetrazolium (NBT) staining for H_2O_2 and $O_2^{\bullet-}$, respectively. Indeed, the *aim1* mutant had relatively low levels of H_2O_2 and $O_2^{\bullet-}$ in the root tip based on the lower intensity of HPF fluorescence and weak NBT staining (Figures 5E to 5H). We also measured H_2O_2 contents in the root tip and found that the H_2O_2 content in *aim1* was lower than that in the wild type (Figure 5I). The reduction in H_2O_2 and $O_2^{\bullet-}$ accumulation in the mutant was restored by introducing the *AIM1* gene driven by the CaMV 35S promoter or its native promoter into the complementation lines

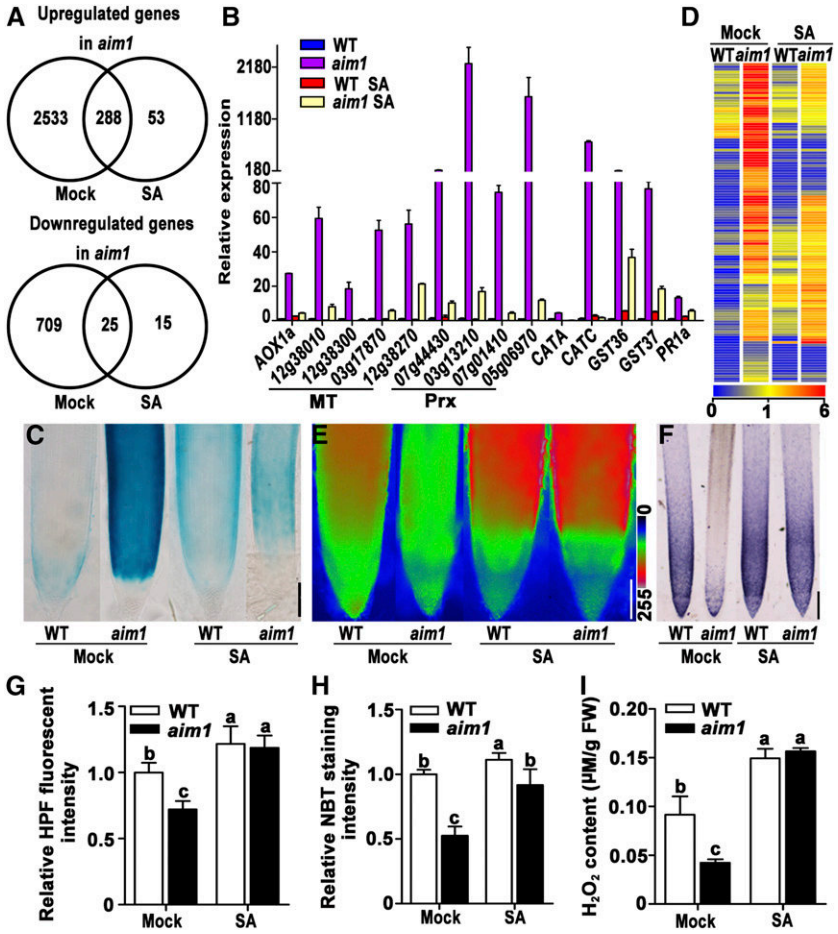

Figure 5. SA Maintains the Expression of Redox and ROS Scavenging-Related Genes for ROS Accumulation in the Root Tip.

(A) Venn diagrams showing transcriptome changes in 4-d-old wild type and *aim1* grown on mock medium and medium supplemented with 0.5 mM SA ($P \leq 0.05$, fold change ≥ 2). The top panel shows the number of upregulated genes in *aim1* under mock or SA treatment. The bottom panel shows the number of downregulated genes in *aim1* under mock or SA treatment.

(B) Relative expression of *AOX1a*, *METALLOTHIONEIN* (*MT*), *PEROXIDASE* (*Prx*), *CATA*, *CATC*, *GST36*, *GST37*, and *PR1a* genes in 4-d-old wild type and *aim1* grown on mock medium and medium supplemented with 0.5 mM SA. The expression level of each gene was compared with that in the wild type grown on mock medium. Total RNA was collected from the 2.5-mm root apex of seedlings. Error bars represent SD ($n = 3$). Three biological replicates were performed per gene. Samples were collected from three independent experiments.

(C) The expression patterns of *ProAOX1a:GUS* in 4-d-old seedlings grown on mock medium and medium supplemented with 0.5 mM SA. Bar = 100 μm.

(D) Heat map of microarray expression profiles for redox and ROS scavenging-related genes. The gradation of colors reflects normalized signal values across the entire array. The "6" indicates high expression, "1" indicates normal expression, and "0" indicates low expression.

(E) Representative pseudo-color images of 4-d-old roots stained with HPF to detect H_2O_2 in the wild type and *aim1* grown on mock medium and medium supplemented 0.5 mM SA. The gradation of colors reflects the intensity of fluorescence. Bar = 100 μm.

(F) $O_2^{\cdot-}$ accumulation revealed by NBT staining in 4-d-old wild type and *aim1* grown on mock medium and medium supplemented with 0.5 mM SA. Bar = 100 μm.

(G) Quantification of HPF fluorescence intensity. Error bars represent SD ($n = 8$). The intensity was compared with that in the wild type grown on mock medium.

(H) Quantification of NBT staining intensity. Error bars represent SD ($n = 8$). The intensity was compared with that in the wild type grown on mock medium.

(I) H_2O_2 contents in root tips (~2.5 mm) of 4-d-old wild type and *aim1* grown on mock medium and medium supplemented with 0.5 mM SA. Error bars represent SD ($n = 3$). Each sample contained ~40 roots. FW, fresh weight. Different letters in **(G)** to **(I)** indicate a significant difference ($P < 0.01$, by Tukey's test).

(Supplemental Figure 7). Since NADPH oxidases catalyze the production of $O_2^{\cdot-}$, we investigated whether the reduced ROS levels in the mutant resulted from the repression of *NADPH oxidase* genes or from the higher rate of ROS scavenging. However, our expression analysis showed that none of the *NADPH oxidase* genes displayed reduced expression in *aim1* (Supplemental Figure 8). Therefore, AIM1 is critical for maintaining ROS levels in the root tip, likely by modulating the expression of redox and ROS scavenging-related genes. To determine whether the alteration in ROS accumulation in *aim1* resulted from defective SA

biosynthesis due to the loss of function of AIM1, we analyzed the effects of SA treatment on ROS accumulation in the wild type and *aim1* mutant. We found that the addition of SA restored ROS accumulation in the *aim1* mutant (Figures 5E to 5I). These results strongly support the hypothesis that AIM1 represses the expression of redox and ROS scavenging-related genes to promote ROS accumulation in rice roots through its critical role in SA biosynthesis.

ROS Act Downstream of SA to Promote Root Meristem Activity in Rice

To investigate whether reduced ROS accumulation in rice leads to a reduction in root meristem activity, we treated wild-type plants with the antioxidants ascorbic acid and glutathione, the primary water-soluble antioxidants in plants. The addition of ascorbic acid or glutathione led to a reduction in both ROS (H_2O_2 and $O_2^{\bullet-}$) accumulation in the root tip and root growth (Figures 6A to 6F). Furthermore, the inhibited root growth after the addition of the antioxidants was associated with reduced root meristem activity based on the reduced number of EdU-labeled cells in the root meristem (Figures 6G and 6H). Ascorbic acid treatment only slightly reduced the root cortical cell length (from 85.12 $\pm$ 5.95 μm to 79.60 $\pm$ 5.78 μm, $n = 30$, $P < 0.01$ by Student's t test), while glutathione treatment had no obvious effect on root cell length. These results indicate that the reduced ROS levels in rice roots specifically inhibit root meristem activity.

To further determine the role of ROS in AIM1-dependent meristem activity in rice roots, we analyzed the effects of exogenously applied H_2O_2 on root growth. We used H_2O_2 because this ROS is relatively stable and can readily diffuse across membranes passively or through water channels (Habibi, 2014). The application of H_2O_2 not only increased the H_2O_2 concentration, but it also restored $O_2^{\bullet-}$ levels in *aim1* root tips (Figures 6K to 6N). Consistent with the restoration of ROS accumulation in the root tip, the exogenous application of H_2O_2 also partially rescued the short root phenotype of *aim1* by increasing the root length of the mutant by ~50% (Figures 6I and 6J). However, the same treatment had no significant impact on root growth in the wild type. Again, the partial restoration of root growth in *aim1* was correlated with the induction of root meristem activity based on increased EdU labeling in the root meristem (Figures 6O and 6P). Collectively, these results indicate that AIM1 in the root is required for the biosynthesis of SA at sufficient levels to repress the expression of redox and ROS scavenging-related genes, thereby increasing ROS accumulation to promote root meristem activity in rice.

SA Inhibits the Expression of Redox and ROS Scavenging-Related Genes Partially through WRKY62 and WRKY76

To determine how in vivo basal SA levels downregulate the expression of redox and ROS scavenging-related genes to maintain proper ROS levels in rice roots, we explored a number of possible molecular mechanisms. NONEXPRESSER OF PR GENES1 (NPR1) and transcription factor WRKY45 are two important regulators of SA signaling in the rice shoot. We found that the expression of *NPR1* in *aim1* was upregulated under both mock and SA treatments (Supplemental Figure 9A). Furthermore, the expression of *WRKY45* was repressed in the *aim1* mutant. Although the exogenous application of SA can induce the expression of *WRKY45* in both the wild type and *aim1* mutant, its transcript level was significantly lower in the *aim1* mutant than in the wild type. These results suggest that NPR1 and WRKY45 might not be the key regulators of the expression of redox and ROS scavenging-related genes in the rice root. As described earlier, a number of PR genes were induced in the *aim1* mutant. Furthermore, rice *WRKY62* and *WRKY76* are induced by SA treatment and function as repressors of PR genes in rice (Liu et al., 2016). To determine whether WRKY62 and WRKY76 also function in SA-regulated root development, we analyzed the expression patterns of *WRKY62* and *WRKY76* in the wild type and *aim1* mutant. Indeed, the transcript levels of *WRKY62* and *WRKY76* were significantly lower in mutant roots than in the wild type (Figure 7A). Consistent with a previous report, SA treatment induced the expression of *WRKY62* and *WRKY76* in both the wild type and, to a greater extent, in the *aim1* mutant. As a result, after SA treatment, the expression levels of the two WRKY genes were similar in the wild type and *aim1* mutant. Thus, reduced SA biosynthesis in *aim1* is associated with reduced levels of *WRKY62* and *WRKY76* expression.

To determine whether the reduced expression of *WRKY62* and *WRKY76* affects the expression of redox and ROS scavenging-related genes, we compared the expression of these genes in the root tip in the wild type and the *WRKY62* and *WRKY76* double knockdown RNAi line (dsOW62/76-108) (Liu et al., 2016). Consistent with a previous report, the expression of *PR1a* was upregulated in dsOW62/76-108. Similarly, a number of genes encoding METALLOTHIONEINs and PEROXIDASEs were upregulated in the dsOW62/76-108 line, although to a lesser extent than in the *aim1* mutant. However, the expression of *CATALASE A* (*CATA*), *CATC*, *GLUTATHIONE S-TRANSFERASE36* (*GST36*), and *GST37* was significantly induced in *aim1* but not in the dsOW62/76-108 line (Figure 7B). These results indicate that the upregulation of redox and ROS scavenging-related genes in the *aim1* mutant is, at least in part, due to reduced expression of *WRKY62* and *WRKY76*.

Given the upregulation of redox and ROS scavenging-related genes, we reasoned that the dsOW62/76-108 line might also be defective in ROS accumulation and root growth. To test this hypothesis, we investigated ROS accumulation and primary root length in the dsOW62/76-108 line. As shown in Figures 7C to 7F, both H_2O_2 and $O_2^{\bullet-}$ accumulation were reduced in the roots of the dsOW62/76-108 line. Furthermore, the primary root length of the double knockdown RNAi line was 20% shorter than that of the wild type (Figures 7G and 7H). Consistent with the short root phenotype, the expression of several cell cycle-related genes was significantly repressed in the double knockdown RNAi line (Figure 7I). To exclude the possibility that the short root phenotype of the double knockdown RNAi line might be due to reduced SA content, as observed in the *aim1* mutant, we determined the SA content in the mutant. The SA content in the dsOW62/76-108 line was slightly higher than that in the wild type (Figure 7J). Thus, the reduced root growth in *aim1* might be due (at least in part) to the reduced expression of *WRKY62* and *WRKY76*, along with the reduced SA accumulation in the mutant. Based on these results, AIM1-dependent SA biosynthesis appears to be required for

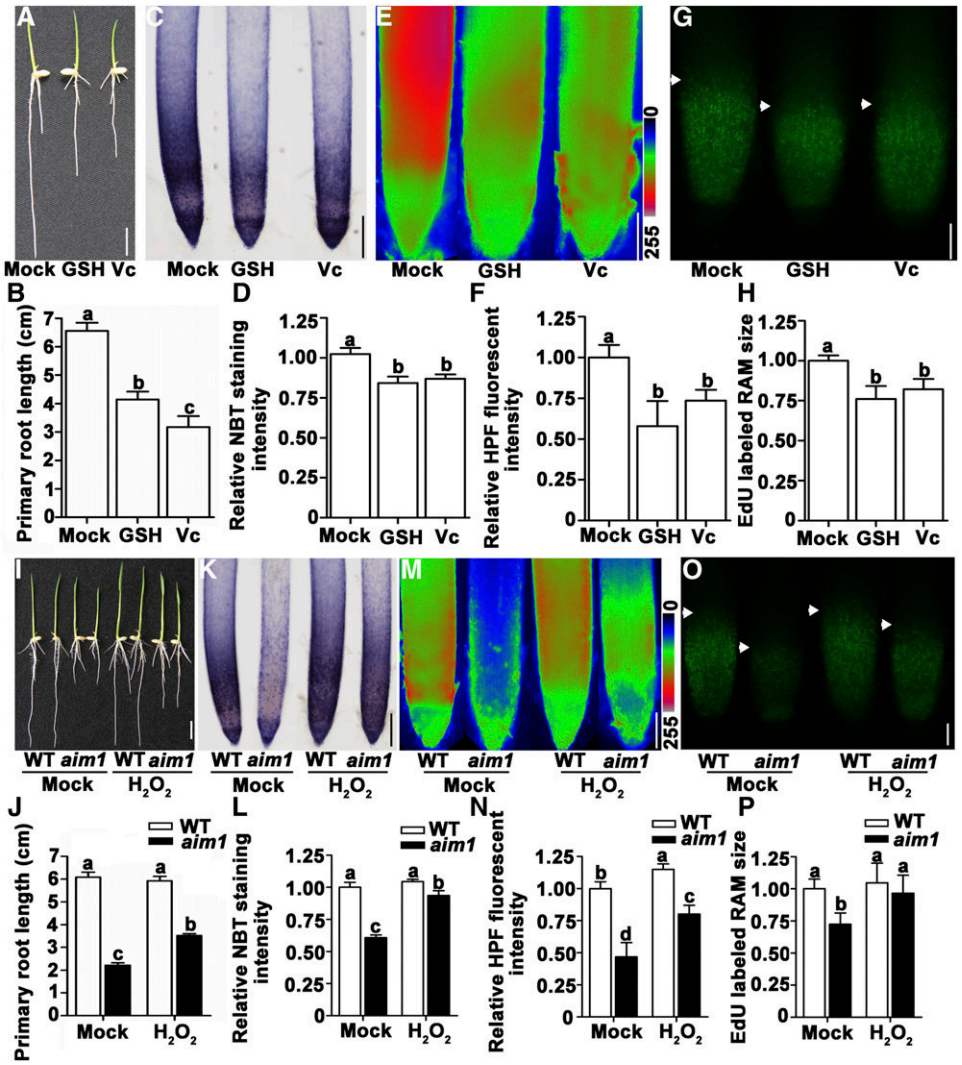

Figure 6. ROS Function Downstream of SA to Maintain Mitotic Activity in Rice Roots.

(A) to **(H)** Exogenous application of antioxidants reduces ROS accumulation in the root tip and inhibits root growth in rice.
(A) Root phenotype of 4-d-old wild type under different treatments. GSH, glutathione (0.5 mM); Vc, ascorbic acid (0.5 mM). Bar = 1 cm.
(B) Primary root length of 4-d-old wild type under different treatments. Error bars represent SD (n = 10).
(C) $O_2^{\bullet-}$ accumulation revealed by NBT staining in 4-d-old wild type under different treatments. Bar = 100 μm.
(D) Quantification of NBT staining intensity. Error bars represent SD (n = 8). The intensity was compared with that in the wild type grown on mock medium.
(E) Pseudo-color images of 4-d-old roots stained with HPF for H_2O_2 in the wild type under different treatments. The gradation of colors reflects the intensity of fluorescence. Bar = 100 μm.
(F) Quantification of HPF fluorescence intensity. Error bars represent SD (n = 8). The intensity was compared with that in the wild type grown on mock medium.
(G) S-phase entry of root tips of 4-d-old wild type visualized by EdU staining. Bar = 100 μm.
(H) Sizes of EdU-labeled RAMs (root apical meristems). Error bars represent SD (n = 8).
(I) to **(P)** H_2O_2 (0.5 mM) can partially rescue the root elongation defect of *aim1*.
(I) Root phenotype of the wild type and *aim1* upon mock and H_2O_2 treatments. Bar = 1 cm.
(J) Primary root length of 4-d-old wild type and *aim1* upon H_2O_2 treatment. Error bars represent SD (n = 8).
(K) $O_2^{\bullet-}$ accumulation revealed by NBT staining in 4-d-old wild type and *aim1* under mock and H_2O_2 treatments. Bar = 100 μm.
(L) Quantification of NBT staining intensity. Error bars represent SD (n = 8). The intensity was compared with that in the wild type grown on mock medium.
(M) Pseudo-color images of 4-d-old roots stained with HPF for H_2O_2 in the wild type and *aim1* under mock and H_2O_2 treatments. The gradation of colors reflects the intensity of fluorescence. Bar = 100 μm.
(N) Quantification of HPF fluorescence intensity. Error bars represent SD (n = 10). The intensity was compared with that in the wild type grown on mock medium.
(O) S-phase entry of root tips of 4-d-old wild type and *aim1* visualized by EdU staining. Bar = 100 μm.
(P) Sizes of EdU-labeled RAMs (root apical meristems). Error bars represent SD (n = 8).
Different letters in **(B)**, **(D)**, **(F)**, **(H)**, **(J)**, **(L)**, **(N)**, and **(P)** indicate a significant difference ($P < 0.01$, by Tukey's test). The arrowheads in **(G)** and **(O)** indicate the border of the EdU staining signal.

the expression of *WRKY62* and *WRKY72*, whose products act as repressors to suppress the expression of redox and ROS scavenging-related genes to increase the accumulation of ROS, which appear to act as signaling molecules to promote root meristem activity in rice.

DISCUSSION

AIM1, a key enzyme for β-oxidation in plants that was first identified in Arabidopsis, plays an important role in inflorescence and floral development (Richmond and Bleecker, 1999). Arabidopsis AIM1 also plays a role in JA and auxin biosynthesis (reviewed in Baker et al., 2006). Here, we identified the *AIM1* homolog in rice and found that rice AIM1 is critical for maintaining root meristem activity. Despite their different roles in plant development, the Arabidopsis and rice AIM1 homologs appear to participate in similar metabolic pathways, including JA biosynthesis in both Arabidopsis and rice. The biochemical conservation and functional variation of AIM1 homologs from different plants suggest significant divergence in the underlying molecular pathways among different plants for the regulation of the growth, development, and responses to changing environments.

In this study, we showed that Os-AIM1-dependent β-oxidation is required for SA biosynthesis in rice. SA in plants can be generated through two distinct pathways: the ISOCHORISMATE SYNTHASE (ICS) pathway and the PHENYLALANINE AMMONIA-LYASE (PAL) pathway. Both pathways require the primary metabolite chorismate. Chorismate-derived L-phenylalanine is catalyzed by PAL to form cinnamic acid, which is then converted to SA via *o*-coumarate or benzoate by β-oxidation, depending on whether the hydroxylation of the aromatic ring takes place before or after the side-chain-shortening reactions. Chorismate can also be converted into SA through two reactions catalyzed by ICS and ISOCHORISMATE PYRUVATE LYASE. The relative contribution, regulation, and coordination of the two pathways in SA biosynthesis are still poorly understood.

The PAL and ICS biosynthetic routes could contribute to the biosynthesis of SA differently in different plant species. Arabidopsis contains low basal levels of SA, and most of pathogen-induced SA is synthesized via the ICS pathway (Wildermuth et al., 2001). The Arabidopsis genome contains two *ICS* genes, both of which contribute to SA biosynthesis, as the *ics1 ics2* double mutant shows greater reduction not only in pathogen- and stress-induced SA accumulation but also in basal SA levels (Garcion et al., 2008). However, residual SA can still be detected in the *ics1 ics2* double mutant, suggesting the presence of an ICS-independent pathway for SA biosynthesis as well in Arabidopsis. Consistent with this possibility, a recent study showed that AIM1 functions in SA biosynthesis in Arabidopsis seeds, supporting a role for the AIM1-dependent β-oxidation functions in the PAL pathway in basal SA biosynthesis (Bussell et al., 2014). Together, these studies indicate that two different pathways might contribute to SA biosynthesis in Arabidopsis. The AIM1-dependent PAL pathway may be responsible for the low basal level of SA biosynthesis, whereas the ICS pathway is responsible a majority of SA biosynthesis in response to biotic and abiotic stress. In contrast to Arabidopsis, rice has relative high basal SA levels. Early feeding studies suggested that CA and BA can be converted into SA in rice shoot tissue (Silverman et al., 1995), and the levels of SA in rice do not respond significantly to pathogen infection. However, none of the genetic components for the conversion of CA and BA into SA have been identified.

We have shown that AIM1 is required for the conversion of CA to BA and contributes to SA biosynthesis in rice. In Arabidopsis, AIM1 hydratase has a preference for short chain acyl-CoAs compared with Arabidopsis MFP2 hydratase (Arent et al., 2010). Consistent with the biochemical preference of AIM1 for the shortening of the side chain of cinnamic acid, we found that the conversion of CA to BA in the *aim1* mutant is substantially reduced compared with the wild type (Supplemental Figure 5B). These results further support the importance of AIM1-dependent β-oxidation in the PAL pathway for SA biosynthesis in rice. However, since there is still residual SA in the *aim1* mutant, and feeding with CA can still induce increases in BA and SA levels in the *aim1* mutant (Supplemental Figures 5B and 5C), other MFPs from the MFP2 subfamily and the ICS pathway may also contribute to the biosynthesis of SA in rice.

We demonstrated that reduced root meristem activity in the rice *aim1* mutant is caused by reduced SA levels. Likewise, transgenic rice expressing the bacterial *nahG* gene (encoding salicylate hydroxylase) displays both reduced SA accumulation and reduced root growth, supporting a role for SA biosynthesis in rice root growth (Kusumi et al., 2006). How SA promotes root elongation in rice has been unclear. Here, we found that in vivo basal SA levels are required to maintain ROS accumulation in the root tip to modulate root meristem activity. Interestingly, in Arabidopsis, UPB1 regulates the expression of *PEROXIDASE* genes and consequently affects the accumulation of superoxide and hydrogen peroxide in the root tip to regulate root meristem activity (Tsukagoshi et al., 2010). Thus, ROS may function as common signaling molecules for root growth in different plants.

ROS also play an important role in other SA-mediated processes. Mutants that accumulate excess SA (such as the SUMO E3 ligase mutant *siz1* and *constitutive expression of pr genes5* mutants) usually accumulate increased ROS levels. By contrast, Arabidopsis *salicylic acid induction deficient2* and *enhanced disease susceptibility4* mutants with compromised SA biosynthesis showed reduced ROS accumulation (Miura et al., 2013; Nie et al., 2015). SA is thought to maintain ROS levels in two different ways. One way is to inhibit the activity of enzymes related to ROS scavenging or mitochondrial function. The binding of CATALASE and ASCORBATE PEROXIDASE (APX) to SA can inhibit their activity, resulting in elevated ROS levels in Arabidopsis and tobacco (*Nicotiana tabacum*) (Durner and Klessig, 1995; Du and Klessig, 1997). In rice roots, CATALASE isozyme activity is also sensitive to SA (Chen et al., 1997). Here, we found that a number of *CATALASE* and *APX* genes were upregulated in the root tip of the *aim1* mutant. Thus, both increased production and reduced inhibition of these ROS-scavenging enzymes may contribute to the reduced ROS levels in the *aim1* mutant due to reduced SA biosynthesis. Our transcriptome profiling also identified additional genes associated with redox and ROS scavenging whose altered expression in the *aim1* mutant could be restored by exogenous SA. Therefore, an important role of SA in regulating cellular redox and ROS accumulation involves its effect on the

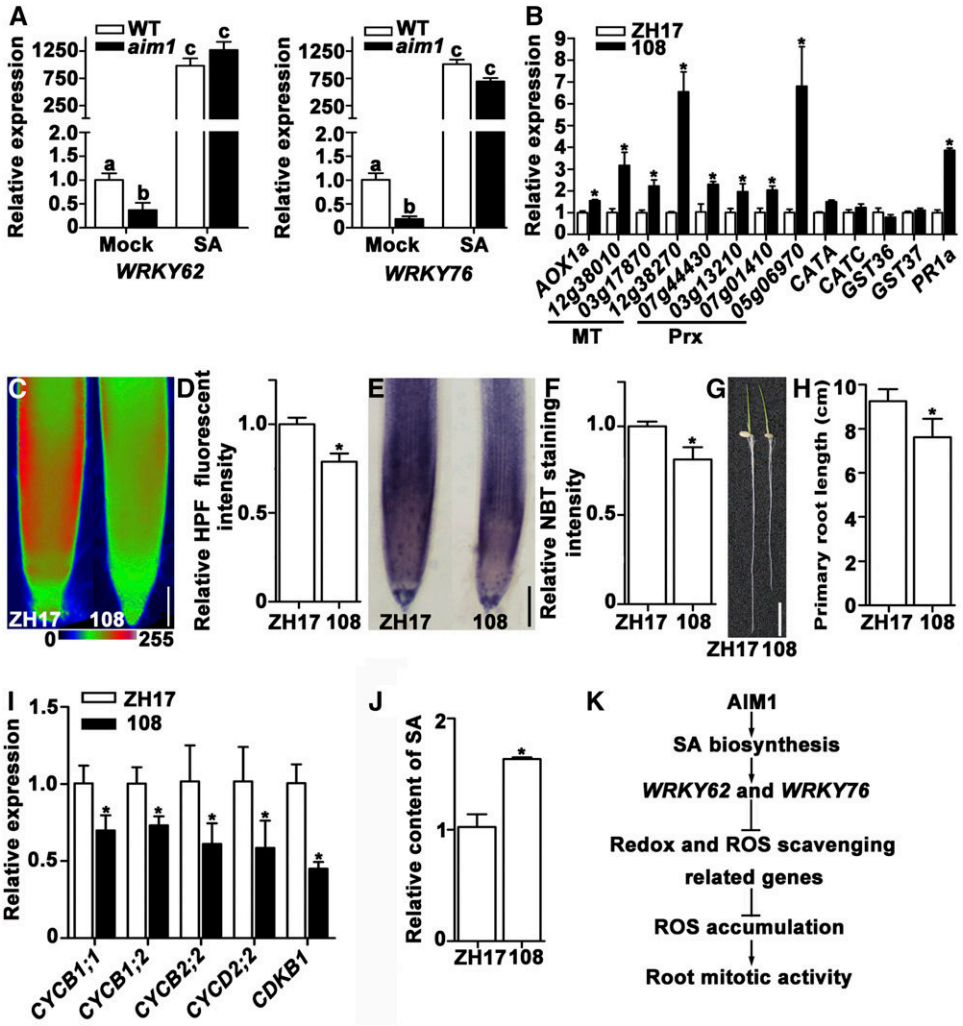

Figure 7. SA Regulates ROS Accumulation and Root Growth, Partially through WRKY62 and WRKY76.

(A) Relative expression of *WRKY62* and *WRKY76* in root tips of 4-d-old wild type and *aim1* grown on mock medium and medium supplemented with 0.5 mM SA based on qRT-PCR. The expression level was compared with that in the wild type grown on mock medium. Error bars represent SD ($n = 3$). Different letters indicate a significant difference ($P < 0.01$, by Tukey's test).

(B) Relative Expression of AOX1a, *METALLOTHIONEIN* (*MT*), *PEROXIDASE* (*Prx*), *CATA*, *CATC*, *GST36*, *GST37*, and *PR1a* genes in root tips of 4-d-old wild type (ZH17) and *WRKY62* and *WRKY76* double knockdown RNAi line dsOW62/76-108 (108). The expression level of each gene in line 108 was compared with that in the wild type. Error bars represent SD ($n = 3$).

(C) Pseudo-color images of 4-d-old roots stained with HPF for H_2O_2 in ZH17 and 108. The gradation of colors reflects the intensity of fluorescence. Bar = 100 μm.

(D) Quantification of HPF fluorescence intensity. Error bars represent SD ($n = 8$). The intensity was compared with that in ZH17.

(E) $O_2^{\bullet-}$ accumulation revealed by NBT staining in 4-d-old ZH17 and 108. Bar = 100 μm.

(F) Quantification of NBT staining intensity. Error bars represent SD ($n = 8$). The intensity was compared with that in ZH17.

(G) Root phenotype of 4-d-old ZH17 and 108. Bar = 1 cm.

(H) Primary root length of 4-d-old ZH17 and 108. Error bars represent SD ($n = 10$).

(I) Relative expression of cell cycle-related genes in root tips of 4-d-old ZH17 and 108. Error bars represent SD ($n = 3$). The expression level of each gene in 108 was compared with that in the wild type.

(J) The relative content of SA in 108 compared with that in ZH17. Error bars represent SD ($n = 3$).

(K) Model of AIM1-dependent regulation of root meristem activity. AIM1-dependent β-oxidation is required for rice root growth due to its critical role in SA biosynthesis. SA maintains root meristem activity by promoting ROS accumulation by inducing WRKY transcriptional repressors, which repress the expression of redox and ROS-scavenging genes.

The asterisk in **(B)**, **(D)**, **(F)**, and **(H)** to **(J)** indicates a significant difference between ZH17 and 108 ($P < 0.01$, by Student's *t* test). Total RNA used in **(A)**, **(B)**, and **(I)** was collected from the 2.5-mm root apex of seedlings. Three biological replicates were performed per gene in **(A)**, **(B)**, and **(I)**. Samples were collected from three independent experiments.

transcription of redox- and ROS-related genes. Similarly, in *Populus*, induced SA elicits potent and sustained oxidative responses, as well as transcriptome reprogramming (Xue et al., 2013).

Our study also identified an important mechanism by which SA upregulates basal ROS levels in rice. We found that SA induces the expression of rice *WRKY62* and *WRKY76*, which encode two WRKY transcriptional repressors. Furthermore, we provide strong evidence that the transcriptional repressors WRKY62 and WRKY76 contribute to the repression of redox and ROS scavenging-related genes in the root tip. Importantly, the double knockdown line for WRKY62 and WRKY76 also displays a short root phenotype. These results support the hypothesis that AIM1-dependent SA biosynthesis suppresses the expression of redox and ROS-scavenging genes to promote ROS accumulation and root meristem activity, at least in part through a transcriptional mechanism for increased production of the transcriptional repressors WRKY62 and WRKY76.

SA, a plant defense signaling molecule, activates the expression of a large number of plant defense genes. Similarly, exogenous application of SA also activates the expression of *PR* genes in rice roots (Figure 5B). However, in contrast to the activation of defense gene expression by exogenous application of SA, we discovered that in vivo basal SA levels repress the expression of redox and ROS scavenging-related genes and some *PR* genes in the rice root. The differential effects of exogenous SA application and in vivo basal SA on gene expression may be explained by the coordination of different transcription activators and repressors. We demonstrated that two SA-induced WRKY transcriptional repressors, WRKY62 and WRKY76, are partly responsible for the repression of redox and ROS scavenging-related genes and *PR* genes. The reduced in vivo SA content in the *aim1* mutant cannot sustain the expression of *WRKY62* and *WRKY76*, which therefore leads to the increased expression of redox and ROS scavenging-related genes. However, exogenous SA application can restore the expression of these two repressors to repress the expression of redox and ROS scavenging-related genes and *PR* genes. In wild-type plants, which have higher basal levels of SA and *WRKY62* and *WRKY76* expression than *aim1*, exogenous application of SA could lead to the preferential induction of other transcriptional activators to modestly induce the expression of redox and ROS scavenging-related genes and *PR* genes (Figure 5).

Contrary to the central role of NPR1 in SA signaling in Arabidopsis, SA signaling in the rice shoot is mediated by NPR1 and the WRKY45 subpathway (Nakayama et al., 2013). We found that the expression of *NPR1* and *WRKY45* in the *aim1* mutant was altered compared with the wild type and that SA application could reduce the differential expression levels of these genes. It would be interesting to determine whether the altered expression of *NPR1* and/or *WRKY45* also contributes to the increased expression of redox and ROS scavenging-related genes in the *aim1* mutant.

In conclusion, we have provided a large body of evidence demonstrating that AIM1-dependent β-oxidation is required for SA biosynthesis in rice. SA biosynthesis in rice roots regulates root meristem activity through maintaining sufficient levels of ROS by suppressing the expression of redox and ROS scavenging-related genes. The suppression of redox and ROS scavenging-related genes by SA is, at least in part, mediated by the transcriptional repressors WRKY62 and WRKY76.

METHODS

Plant Materials and Growth Conditions

The rice (*Oryza sativa*) mutant *aim1* was identified from a ^{60}Coγ-ray radiation mutagenized population derived from the japonica cultivar 'Shishoubaimao'. Hydroponic experiments were conducted using a modified rice culture solution containing 1.425 mM NH_4NO_3, 0.2 mM NaH_2PO_4, 0.513 mM K_2SO_4, 0.998 mM $CaCl_2$, 1.643 mM $MgSO_4$, 0.009 mM $MnCl_2$, 0.075 mM $(NH_4)_6Mo_7O_{24}$, 0.019 mM H_3BO_3, 0.155 mM $CuSO_4$, and 0.152 mM $ZnSO_4$ with 0.125 mM EDTA-Fe. The pH of the solution was adjusted to 5.5. All plants were grown in a greenhouse with a 12-h-day (30°C)/12 h night (22°C) photoperiod, ~200 μmol m^{-2} s^{-1} photon density, and ~60% humidity. Light (500–700 nm) was provided by Philips HPI Plus BU bulbs. For SA treatment, SA stock solution (100 mM) was freshly prepared. For methyl salicylate, H_2O_2 (0.5 mM), GSH (0.5 mM), and ascorbic acid (0.5 mM) treatment, the chemicals were added to the culture solution directly. For JA and DIECA treatment, JA (100 mM) and DIECA (100 mM) stock solution were freshly prepared. For CA and BA treatment, CA (200 mM) and BA (200 mM) stock solution were freshly prepared.

Histological Observation

To produce longitudinal sections of roots, root tips were fixed overnight at 4°C in 2.5% glutaraldehyde in 0.1 M sodium phosphate buffer, pH 7.2, and washed three times for 30 min in the same buffer. Root samples were then fixed for 4 h in 1% OsO_4 in 0.1 M sodium phosphate buffer, pH 7.2, and washed for 30 min in the same buffer. The samples were dehydrated in a gradient ethanol series and embedded in Spurr's resin. Semithin sections (2 μm thick) were produced using a Power Tome XL microtome and stained in 0.1% methylene blue for 3 to 5 min at 70°C. The samples were rinsed with distilled water and visualized under a microscope (Nikon ECLIPSE Ni).

To produce transverse sections of roots, root segments were embedded in 3% agar. Transverse sections (30 μm) of root were produced using a vibratome (Leica VT 1000 S). The images of rice root autofluorescence were taken under a microscope (Nikon ECLIPSE Ni). The images were processed with ImageJ software.

Map-Based Cloning of *Osaim1*

For positional cloning of the mutated gene, *aim1* was crossed with Kasalath, an indica rice variety, to generate an F2 mapping population. Based on bulked segregant analysis, the *AIM1* gene was mapped to the short arm of chromosome 2 between marker S2-9925K and S2-10093K using 600 F2 mutant plants. The mutated gene was identified via sequencing the genes between the two markers.

Plasmid Construction and Plant Transformation

Sequence information for the primers used to construct the vectors is shown in Supplemental Table 4. To generate complementation vectors, the coding region of *AIM1* was amplified from rice cDNA and inserted into the *Xba*I and *Pst*I sites in the pCAMBIA 1300 vector. For the *ProAIM1:AIM1* vector, the 3000-bp native promoter sequence before the start codon was introduced into the *Kpn*I and *Xba*I sites upstream of the *AIM1* coding region. For the *Pro35S:AIM1* vector, the coding region of *AIM1* was introduced into the *Kpn*I and *Sal*I sites downstream of the 35S promoter. The *ProAIM1:GUS-AIM1* vector was generated by inserting the GUS fragment into the *Xba*I site on the *ProAIM1:AIM1* vector. To generate the *Pro35S:GFP-AIM1* vector, the GFP fragment was inserted into the *Pro35S:AIM1* vector. To generate the *ProAOX1a:GUS* vector, the GUS fragment was inserted into the *Sac*I and *Eco*RI sites on the pCAMBIA

1300 vector, and the 1200-bp promoter sequence of *AOX1a* was then inserted into the *Bam*HI and *Kpn*I sites upstream of *GUS*.

The constructs were transformed into mature embryos developed from seeds of the wild type ('Shishoubaimao') via *Agrobacterium tumefaciens*-mediated transformation as described (Deng et al., 2014).

Histochemical Localization of GUS Expression

For GUS staining, the tissues were incubated in a solution containing 50 mM sodium phosphate buffer (pH 7.0), 5 mM $K_3Fe(CN)_6$, 5 mM $K_4Fe(CN)_6$, 0.1% Triton X-100, and 1 mM X-Gluc at 37°C. Sections (35 μm) of various plant tissues were produced using a vibratome (Leica VT 1000 S). Images were taken under a microscope (Nikon ECLIPSE Ni).

Microarray Analysis

Total RNA was isolated from primary root tips (~2.5 mm) of 4-d-old wild-type and *aim1* plants treated with mock or 0.5 mM SA. Two biological replicates were performed. Samples were collected from two independent experiments. Total RNA was isolated using an RNeasy plant mini kit (Qiagen). Samples were submitted for hybridization to the rice whole genome Affymetrix GeneChip. Microarray data analyses were performed as previously described (Bustos et al., 2010). GO classification analysis was performed with agriGO (http://bioinfo.cau.edu.cn/agriGO).

Quantitative RT-PCR

Reverse transcription was performed using 2 μg of total RNA and M-MuLV reverse transcriptase (NEB) according to the manufacturer's instructions. Quantitative PCR (qPCR) was performed using the Roche SYBR Green I kit on a LightCycler480 machine (Roche Diagnostics) according to the manufacturer's instructions. Three biological replicates were performed per gene. Three technical replicates were performed per gene within an experiment. Samples were collected from three independent experiments. The rice *Actin* gene was used as an internal control. The primers used for qRT-PCR are listed in Supplemental Table 4.

NBT and HPF Staining

Rice roots were stained for 30 min in a solution of 2 mM NBT or 5 μM HPF in 20 mM phosphate buffer (pH 6.1). The reaction was stopped by transferring the seedlings to distilled water. Root tips were imaged under bright-field illumination for NBT staining or GFP channel for HPF staining using a Nikon microscope. The intensity of NBT and HPF staining was quantified using ImageJ software.

Subcellular Localization Analysis

Rice shoot protoplasts were obtained and transformed with *Pro35S:GFP-AIM1* and the peroxisome targeting fluorescent protein (mCherry-PTS1) marker construct according to Zhang et al. (2011). Fluorescence imaging of the protoplasts was performed using a confocal laser scanning microscope (SP5; Leica Microsystems).

EdU Staining

EdU staining was performed using an EdU kit (C10350, Click-iT EdU Alexa Fluor 488 HCS assay; Invitrogen), according to the manufacturer's protocol. Roots of 4-d-old rice seedlings were immersed in 20 μM EdU solution for 2 h and fixed for 30 min in 3.7% formaldehyde solution in phosphate buffer (pH 7.2) with 0.1% Tritonx-100, followed by 30 min of incubation with EDU detection cocktail. The images were captured with the GFP channel on a Nikon microscope.

H_2O_2 Measurement

H_2O_2 content was measured using an Amplex Red Hydrogen Peroxide assay kit (Invitrogen) following the vendor's instructions. For sample preparation, 2.5 mm root tips of 4-d-old seedlings were ground in liquid nitrogen and thoroughly mixed with 3 volumes of H_2O by vigorous vortexing. After centrifugation at 12,000 rpm for 20 min at 4°C, the supernatants were used for the H_2O_2 assay.

Metabolite Measurements

For metabolite measurements, seedlings were grown in culture solution for two weeks. The aerial parts and roots were separately collected and freeze-dried. The freeze-dried tissues were used for metabolite measurements following previously published methods (Chen et al., 2013). The sample extracts were analyzed using an LC-ESI-MS/MS system (HPLC, Shim-pack UFLC Shimadzu CBM20A system; MS, Applied Biosystems 4000 Q TRAP).

Phylogenetic Analysis

The protein sequences of MFPs from different species were retrieved from PLAZA (http://bioinformatics.psb.ugent.be/plaza/). Alignment of the MFPs is presented in Supplemental File 1. Phylogenetic analysis was conducted with CIPRES (www.phylo.org) using maximum-likelihood phylogenetic analysis with 1000 bootstrap replicates. Parameter settings were as follows: mLsearch, ture; no_bfgs, false; printbrlength, false; prot_matrix_spec, JTT; use_bootstopping, true. *Chlamydomonas reinhardtii* AIM was used as an outgroup.

Accession Numbers

Sequence data from this article can be found in the Rice Genome Annotation Project (http://rice.plantbiology.msu.edu/) under accession numbers Os02g17390 (*AIM1*), Os03g50885 (*ACTIN*), Os09g25060 (*WRKY76*), Os09g25070 (*WRKY62*), and Os04g51150 (*AOX1a*). The microarray data from this study can be found in Gene Expression Omnibus under accession number GSE80184.

Supplemental Data

Supplemental Figure 1. Root and panicle phenotypes of *aim1* and quantification of root length and *AIM1* expression in the complementation lines.

Supplemental Figure 2. Relative expression of MFP genes in different organs of 15-d-old wild-type plants.

Supplemental Figure 3. The GUS-AIM1 fusion driven by its native promoter completely rescues the root growth defects in *aim1*.

Supplemental Figure 4. The short root defect of *aim1* does not result from compromised JA biosynthesis.

Supplemental Figure 5. AIM1 is involved in the conversion of CA to BA, which subsequently affects SA biosynthesis in rice.

Supplemental Figure 6. Exogenous application of salicylic acid or methyl salicylate rescues the root growth defects of *aim1*.

Supplemental Figure 7. The reduction in H_2O_2 and $O_2^{\bullet-}$ accumulation in the mutant is rescued by the expression of *AIM1* driven by the CaMV 35S promoter or its native promoter in the complementation lines.

Supplemental Figure 8. Relative expression of *NADPH oxidase* genes in 4-d-old wild type and *aim1*.

Supplemental Figure 9. Relative expression of *WRKY45* and *NPR1* in 4-d-old wild type and *aim1* grown on mock medium and medium supplemented with 0.5 mM SA.

Supplemental Table 1. Enriched Gene Ontology categories among genes that are AIM1 dependent or AIM1 repressed.

Supplemental Table 2. List of cyclin genes whose expression is reduced in the *aim1* mutant and induced by SA application in the *aim1* background to levels similar to those in the wild type.

Supplemental Table 3. List of PR genes whose expression is induced in the *aim1* mutant and reduced by SA application in the *aim1* background to levels similar to those in the wild type.

Supplemental Table 4. Primer sequences used in this study.

Supplemental File 1. Protein sequence alignment of MFPs.

ACKNOWLEDGMENTS

We thank Zejiang Guo for providing the *WRKY62* and *WRKY76* double knockdown mutant. This work was supported by the National Key Research and Development Program of China (2016YFD0100700) and the National Natural Science Foundation (31322048, 31272227, and 31200154). K.Y. was supported by the National Program for the Support of Top-notch Young Professionals and the Innovation Program of Chinese Academy of Agricultural Sciences.

AUTHOR CONTRIBUTIONS

K.Y. conceived and supervised the project. L.X. and K.Y. designed the research. L.X., H.Z., W.R., M.D., and F.W. performed the experiments. L.X., H.Z., W.R., M.D., F.W., J.P., J.L., Z.C., and K.Y. analyzed data. L.X. and K.Y. wrote the article with contributions from all the authors.

Received August 24, 2016; revised February 28, 2017; accepted March 10, 2017; published March 14, 2017.

REFERENCES

Arent, S., Christensen, C.E., Pye, V.E., Nørgaard, A., and Henriksen, A. (2010). The multifunctional protein in peroxisomal beta-oxidation: structure and substrate specificity of the *Arabidopsis thaliana* protein MFP2. J. Biol. Chem. **285:** 24066–24077.

Baker, A., Graham, I.A., Holdsworth, M., Smith, S.M., and Theodoulou, F.L. (2006). Chewing the fat: beta-oxidation in signalling and development. Trends Plant Sci. **11:** 124–132.

Bussell, J.D., Reichelt, M., Wiszniewski, A.A., Gershenzon, J., and Smith, S.M. (2014). Peroxisomal ATP-binding cassette transporter COMATOSE and the multifunctional protein abnormal INFLORESCENCE MERISTEM are required for the production of benzoylated metabolites in Arabidopsis seeds. Plant Physiol. **164:** 48–54.

Bustos, R., Castrillo, G., Linhares, F., Puga, M.I., Rubio, V., Pérez-Pérez, J., Solano, R., Leyva, A., and Paz-Ares, J. (2010). A central regulatory system largely controls transcriptional activation and repression responses to phosphate starvation in Arabidopsis. PLoS Genet. **6:** e1001102.

Chen, Q., et al. (2011). The basic helix-loop-helix transcription factor MYC2 directly represses PLETHORA expression during jasmonate-mediated modulation of the root stem cell niche in Arabidopsis. Plant Cell **23:** 3335–3352.

Chen, W., Gong, L., Guo, Z., Wang, W., Zhang, H., Liu, X., Yu, S., Xiong, L., and Luo, J. (2013). A novel integrated method for large-scale detection, identification, and quantification of widely targeted metabolites: application in the study of rice metabolomics. Mol. Plant **6:** 1769–1780.

Chen, Z., Iyer, S., Caplan, A., Klessig, D.F., and Fan, B. (1997). Differential accumulation of salicylic acid and salicylic acid-sensitive catalase in different rice tissues. Plant Physiol. **114:** 193–201.

Deng, M., Hu, B., Xu, L., Liu, Y., Wang, F., Zhao, H., Wei, X., Wang, J., and Yi, K. (2014). OsCYCP1;1, a PHO80 homologous protein, negatively regulates phosphate starvation signaling in the roots of rice (*Oryza sativa* L.). Plant Mol. Biol. **86:** 655–669.

Du, H., and Klessig, D.F. (1997). Identification of a soluble, high-affinity salicylic acid-binding protein in tobacco. Plant Physiol. **113:** 1319–1327.

Dunand, C., Crèvecoeur, M., and Penel, C. (2007). Distribution of superoxide and hydrogen peroxide in Arabidopsis root and their influence on root development: possible interaction with peroxidases. New Phytol. **174:** 332–341.

Durner, J., and Klessig, D.F. (1995). Inhibition of ascorbate peroxidase by salicylic acid and 2,6-dichloroisonicotinic acid, two inducers of plant defense responses. Proc. Natl. Acad. Sci. USA **92:** 11312–11316.

Galinha, C., Hofhuis, H., Luijten, M., Willemsen, V., Blilou, I., Heidstra, R., and Scheres, B. (2007). PLETHORA proteins as dose-dependent master regulators of Arabidopsis root development. Nature **449:** 1053–1057.

Garcion, C., Lohmann, A., Lamodière, E., Catinot, J., Buchala, A., Doermann, P., and Métraux, J.P. (2008). Characterization and biological function of the ISOCHORISMATE SYNTHASE2 gene of Arabidopsis. Plant Physiol. **147:** 1279–1287.

Goepfert, S., and Poirier, Y. (2007). Beta-oxidation in fatty acid degradation and beyond. Curr. Opin. Plant Biol. **10:** 245–251.

Habibi, G. (2014). Hydrogen peroxide (H_2O_2) generation, scavenging and signaling in plants. In Oxidative Damage to Plants, P. Ahmad, ed (San Diego, CA: Academic Press), pp. 557–584.

Hassinen, V.H., Tervahauta, A.I., Schat, H., and Kärenlampi, S.O. (2011). Plant metallothioneins–metal chelators with ROS scavenging activity? Plant Biol. (Stuttg.) **13:** 225–232.

Joo, J.H., Bae, Y.S., and Lee, J.S. (2001). Role of auxin-induced reactive oxygen species in root gravitropism. Plant Physiol. **126:** 1055–1060.

Kotogány, E., Dudits, D., Horváth, G.V., and Ayaydin, F. (2010). A rapid and robust assay for detection of S-phase cell cycle progression in plant cells and tissues by using ethynyl deoxyuridine. Plant Methods **6:** 5.

Kusumi, K., Yaeno, T., Kojo, K., Hirayama, M., Hirokawa, D., Yara, A., and Iba, K. (2006). The role of salicylic acid in the glutathione-mediated protection against photooxidative stress in rice. Physiol. Plant. **128:** 651–661.

Liszkay, A., van der Zalm, E., and Schopfer, P. (2004). Production of reactive oxygen intermediates ($O_2^{\bullet-}$, H_2O_2, and ·OH) by maize roots and their role in wall loosening and elongation growth. Plant Physiol. **136:** 3114–3123, discussion 3001.

Liu, J., Chen, X., Liang, X., Zhou, X., Yang, F., Liu, J., He, S.Y., and Guo, Z. (2016). Alternative splicing of rice WRKY62 and WRKY76 transcription factor genes in pathogen defense. Plant Physiol. **171:** 1427–1442.

Maxwell, D.P., Wang, Y., and McIntosh, L. (1999). The alternative oxidase lowers mitochondrial reactive oxygen production in plant cells. Proc. Natl. Acad. Sci. USA **96:** 8271–8276.

Miura, K., Okamoto, H., Okuma, E., Shiba, H., Kamada, H., Hasegawa, P.M., and Murata, Y. (2013). SIZ1 deficiency causes reduced stomatal aperture and enhanced drought tolerance via controlling salicylic acid-induced accumulation of reactive oxygen species in Arabidopsis. Plant J. **73:** 91–104.

Nakayama, A., Fukushima, S., Goto, S., Matsushita, A., Shimono, M., Sugano, S., Jiang, C.J., Akagi, A., Yamazaki, M., Inoue, H., and Takatsuji, H. (2013). Genome-wide identification of WRKY45-regulated genes that mediate benzothiadiazole-induced defense responses in rice. BMC Plant Biol. **13:** 150.

Nelson, B.K., Cai, X., and Nebenführ, A. (2007). A multicolored set of in vivo organelle markers for co-localization studies in Arabidopsis and other plants. Plant J. **51:** 1126–1136.

Nie, S., Yue, H., Zhou, J., and Xing, D. (2015). Mitochondrial-derived reactive oxygen species play a vital role in the salicylic acid signaling pathway in *Arabidopsis thaliana*. PLoS One **10:** e0119853.

Pacifici, E., Polverari, L., and Sabatini, S. (2015). Plant hormone cross-talk: the pivot of root growth. J. Exp. Bot. **66:** 1113–1121.

Richmond, T.A., and Bleecker, A.B. (1999). A defect in beta-oxidation causes abnormal inflorescence development in Arabidopsis. Plant Cell **11:** 1911–1924.

Rylott, E.L., Eastmond, P.J., Gilday, A.D., Slocombe, S.P., Larson, T.R., Baker, A., and Graham, I.A. (2006). The *Arabidopsis thaliana* multifunctional protein gene (MFP2) of peroxisomal beta-oxidation is essential for seedling establishment. Plant J. **45:** 930–941.

Sabatini, S., Beis, D., Wolkenfelt, H., Murfett, J., Guilfoyle, T., Malamy, J., Benfey, P., Leyser, O., Bechtold, N., Weisbeek, P., and Scheres, B. (1999). An auxin-dependent distal organizer of pattern and polarity in the Arabidopsis root. Cell **99:** 463–472.

Sánchez-Fernández, R., Fricker, M., Corben, L.B., White, N.S., Sheard, N., Leaver, C.J., Van Montagu, M., Inzé, D., and May, M.J. (1997). Cell proliferation and hair tip growth in the Arabidopsis root are under mechanistically different forms of redox control. Proc. Natl. Acad. Sci. USA **94:** 2745–2750.

Scandalios, J.G., Guan, L., and Polidoros, A.N. (1997). Catalases in plants: gene structure, properties, regulation, and expression. In Oxidative Stress and the Molecular Biology of Antioxidant Defences, J.G. Scandalios, ed (Cold Spring Harbor, NY: Cold Spring Harbor Laboratory Press), pp. 343–406.

Silverman, P., Seskar, M., Kanter, D., Schweizer, P., Metraux, J.P., and Raskin, I. (1995). Salicylic acid in rice (biosynthesis, conjugation, and possible role). Plant Physiol. **108:** 633–639.

Tsukagoshi, H., Busch, W., and Benfey, P.N. (2010). Transcriptional regulation of ROS controls transition from proliferation to differentiation in the root. Cell **143:** 606–616.

Wildermuth, M.C., Dewdney, J., Wu, G., and Ausubel, F.M. (2001). Isochorismate synthase is required to synthesize salicylic acid for plant defence. Nature **414:** 562–565.

Xue, L.J., Guo, W., Yuan, Y., Anino, E.O., Nyamdari, B., Wilson, M.C., Frost, C.J., Chen, H.Y., Babst, B.A., Harding, S.A., and Tsai, C.J. (2013). Constitutively elevated salicylic acid levels alter photosynthesis and oxidative state but not growth in transgenic populus. Plant Cell **25:** 2714–2730.

Yu, X., et al. (2013). Plastid-localized glutathione reductase2-regulated glutathione redox status is essential for Arabidopsis root apical meristem maintenance. Plant Cell **25:** 4451–4468.

Zhang, Y., Su, J., Duan, S., Ao, Y., Dai, J., Liu, J., Wang, P., Li, Y., Liu, B., Feng, D., Wang, J., and Wang, H. (2011). A highly efficient rice green tissue protoplast system for transient gene expression and studying light/chloroplast-related processes. Plant Methods **7:** 30.